

Dynamic Mechanical Properties of Conductive Carbon Black-Reinforced Closed Cell Microcellular Oil-Extended EPDM Rubber Vulcanizates: Effect of Blowing Agent, Temperature, Frequency, and Strain

S. P. Mahapatra, D. K. Tripathy

Rubber Technology Centre, Indian Institute of Technology, Kharagpur 721302, India

Received 28 July 2005; accepted 18 November 2005

DOI 10.1002/app.23927

Published online in Wiley InterScience (www.interscience.wiley.com).

ABSTRACT: Dynamic viscoelastic properties of Vulcan XC 72 (excess conductive carbon black)-reinforced solid- and closed-cell microcellular controlled long chain branching grade oil-extended EPDM (Keltan 7341A) rubber vulcanizates were studied at four frequencies of 3.5, 11, 35, and 110 Hz, and at a temperature range of -100 to 160°C . The effect of blowing agent (ADC 21) loading on storage modulus (E') and loss tangent ($\tan \delta$) was studied. The log of storage modulus bears a linear relationship with the log of density for both solid and microcellular rubber. Relative storage modulus (E'_r/E'_s) decreases with decrease in relative density (ρ_r/ρ_s). Both E' and $\tan \delta$ were found to be dependent on frequency and temperature. The master curves of the stor-

age modulus versus log temperature-reduced frequency were formed by superimposing E' results and by using shift factors calculated by Arrhenius equation. Strain-dependent isothermal dynamic viscoelastic properties were carried out for dynamic strain amplitude of 0.08–7%. Cole–Cole plots of microcellular vulcanizates show a circular arc with blowing agent (density). Empirical relationship between $\tan \delta$ versus E' is found to be linear, whose slope is independent of blowing agent loading or density. © 2006 Wiley Periodicals, Inc. *J Appl Polym Sci* 102: 1600–1608, 2006

Key words: microcellular elastomers; dynamic mechanical properties; blowing agent; density; conductive carbon black

INTRODUCTION

Dynamic mechanical analysis of closed cell microcellular rubber is an important tool to study the viscoelastic behavior of the material, for evaluation of its use in various engineering applications. Microcellular ethylene–propylene–diene terpolymer (EPDM), especially a conjugated long chain branching (CLCB) grade rubber vulcanizates filled with excess conductive carbon black, is widely used as electrostatic charge dissipate material in pressure sensitive sensor, transducer, electromagnetic interference shielding material, and as packaging material in electronics, aircraft, and telecommunications. The dynamic viscoelastic response of closed cell microcellular EPDM rubber plays an important role in packaging, sealing, and vibration isolation applications, because of its lightweight, better design flexibility, excellent weathering, and ageing characteristics. Studies on physical, mechanical, and dynamic mechanical properties of cellular elastomers as well as thermoplastics have been reported earlier.^{1–10}

The linear relation between log shear modulus and log density of closed cell microcellular EPDM¹ and

polyurethane foams^{2,3} has been reported by researchers. The values of storage modulus have been shown as follows:

$$\text{Storage modulus } (E') = a\rho^b \quad (1)$$

where a and b are the constants at a particular temperature and vary with the change of temperature, and ρ is the density. Turner et al.⁴ studied the dynamic mechanical response of flexible polyurethane foam specimens as well as of compression-molded plaque of the same material and characterized the morphological structure in the foam. Kosten and Zwickwer⁵ theoretically studied the pneumatic damping of open cell foam. Gent and Rusch⁶ studied the resistance of open cell polyurethane foam to airflow and permeability. They also described a model for viscoelastic behavior of open cell foams.⁷ Rinde and Hoge^{8,9} constructed the master curve of dynamic shear modulus of polystyrene bead foams and solid polymer for different frequencies as well as for a wide range of temperatures. The linear elastic properties of microcellular plastics have been reported by Jackson et al.¹⁰ Strain-dependent dynamic mechanical properties of solid rubbers are reported by several workers,^{11–20} whereas very little work on closed cell microcellular rubbers has been investigated. The studies on the vis-

Correspondence to: D. K. Tripathy (dkt@rtc.iitkgp.ernet.in).

TABLE I
Formulations of Vulcan XC72-Filled Vulcanizates

	EB ₅	EB ₆	EB ₇	EB ₈
Keltan 7341A (parts in grams)	120	120	120	120
Vulcan XC72 (parts in grams)	40	40	40	40
Paraffinic oil (parts in grams)	4	4	4	4
ADC-21 (parts in grams)	0	2	4	6

Each mix contains ZnO (5 phr), stearic acid (1.5 phr), and dicumyl peroxide (1 phr, 98% pure).

coelastic behaviors of closed cell microcellular ethylene-octene copolymer²¹⁻²³ show that the storage modulus and $\tan \delta$ (the ratio of loss modulus and storage modulus) are frequency- and temperature-dependent, and the log of storage modulus bears a linear relationship with the log of density.

The morphology, physicochemical properties, compressive deformation, and energy absorption characteristics of closed cell microcellular EPDM (Keltan 7341 A), filled with excess conductive carbon black (Vulcan XC 72), have been reported,^{24,25} recently, which describes the effect of filler and blowing agent on the aforementioned properties.

The objective of the present work is to study the dynamic viscoelastic properties of excess conductive carbon black (Vulcan XC 72)-reinforced CLCB grade oil-extended EPDM (Keltan 7341 A)-based closed cell microcellular rubber vulcanizates. The effects of blowing agent (density), temperature, and frequency on dynamic viscoelastic properties of the vulcanizates were studied. The strain-dependent isothermal dynamic mechanical properties of the vulcanizates were also studied.

EXPERIMENTAL

Materials

An oil-extended EPDM rubber [Keltan 7341A, (a new CLCB grade rubber) ethylene-norbornene 7.5 wt %, oil 20 phr, Mooney viscosity 53 (at 150°C), manufactured by DSM Elastomers, Singapore] was used. Vulcan XC72 (excess conductive carbon black) was used as filler, supplied by Cabot Corp., USA. The curative used was dicumyl peroxide, with a purity of 98%, manufactured by Aldrich Chemical Company (Milwaukee, WI). The blowing agent used was azo dicarbonamide, manufactured by High Polymer Lab, India, and Paraffinic oil used was Sunpar oil, supplied by Sun Oil Company, Kolkata.

Sample preparation

The rubber was compounded with the ingredients, according to the formulations of the mixes given in Table I, and the blowing agent was loaded at the end. Compounding was done in a laboratory size

two roll mixing mill at room temperature, according to ASTM D 3182. Cure and blowing characteristics of the compounds were determined in a Monsanto Rheometer, R-100. The vulcanizates were press-molded at 160°C to 80% of their respective cure times to obtain a closed cell microcellular sheet. All sides of the mold were tampered to 30°, to facilitate the expansion of the molded compounds to closed cell, nonintercommunicating microcellular products with a better mold-release. As the press is closed, the compounds completely fill the mold, expelling the air and sealing the cavity. The typical compound flows readily in the molds, coalesces, and eliminates trapped air blisters. As the stock temperature increases, the cure starts, and the decomposition of the blowing agent begins. Carbon dioxide is released, and the cell starts to form. As the decomposition progresses, an exotherm develops and pressure builds up. These factors accelerate the curing rate. The press is opened before the cure has been completed. A very small closed cell is obtained after expansion. The precured sheet was then postcured at 100°C (for 1 h) to complete the curing. The scanning electron microscopy (SEM) photomicrographs of razor-cut surface of 40 phr Vulcan XC 72-filled microcellular Keltan 7341A are shown in Figure 1, with 4 and 6 phr blowing agent loading.

Testing

Dynamic mechanical properties of microcellular Keltan 7341A rubber vulcanizates reinforced with Vulcan XC 72 were studied as a function of temperature and strain with the help of the Rheovibron DDV III EP of Orientec Corp., Japan. Test pieces were in strip-form, with approximate dimensions of 6.0 × 0.3 × 0.5 (all are in centimeters). Tests were carried out at four frequencies (3.5, 11, 35, and 110 Hz) over a wide range of temperatures from -100 to 160°C, with a dynamic strain of 0.18%. For measurement of strain-dependent dynamic mechanical properties, all tests were carried out at 30 ± 2 °C and at a frequency of 11 Hz. The test piece length was varied so as to cover a range of dynamic strain amplitude (DSA) from 0.08 to 7%. DSA is defined as the ratio of peak-to-peak deformation (total excursion path) of the sample to the length of the sample. Mathematically, DSA is $2\Delta L/L_0$, where ΔL is the strain and L_0 is the length of the test piece.

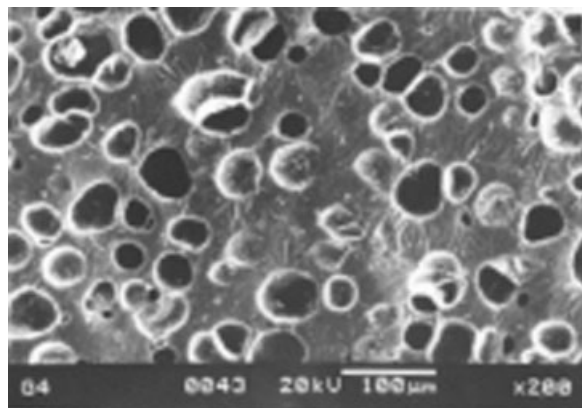
Density of the samples was measured by gravimetric method.

RESULTS AND DISCUSSION

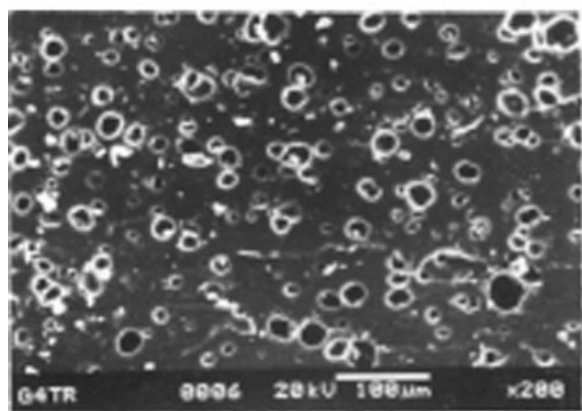
Temperature-dependent dynamic properties

Effect of blowing agent

Figure 2 shows the variation of storage modulus E' , at 11 Hz, with temperature for 40 phr Vulcan XC 72-



(a)



(b)

Figure 1 SEM photomicrographs of razor-cut surfaces of 40 phr Vulcan XC 72-filled microcellular Keltan 7341A (oil-extended EPDM) vulcanizates. (a) EB₇ (4 phr blowing agent); (b) EB₈ (6 phr blowing agent).

filled closed cell microcellular EPDM rubber vulcanizates, with different blowing agent loadings. The nature of storage modulus–temperature curve of closed cell microcellular rubber is similar to that of solid rubber. In glassy region (below glass transition temperature), E' decreases with the increase in blowing agent loadings. The decomposed gas is enclosed in closed cells. The deformation of enclosed gas in closed cell is elastic in nature and has little effect on the storage modulus.⁹ Hence, E' decreases continuously with increase in blowing agent loading because of the decrease in solid rubber content, that is, with decreasing density.

The logarithmic of storage modulus of solid and microcellular rubber vulcanizates are plotted against density at four different temperatures (-100 , -50 , 50 , and 100°C) in Figure 3. From the plot, a linear relationship is evident which obeys the relationship in eq. (1). In the plot, a and b are constants at a particular temperature and vary with the change of temperature, and ρ is the density, the values of which at -100 , -50 ,

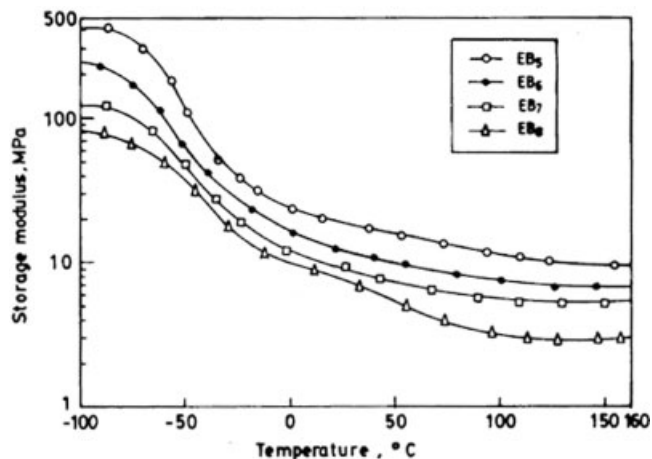


Figure 2 Plots of storage modulus versus temperature of 40 phr Vulcan XC 72-filled microcellular oil-extended EPDM vulcanizates: Effect of blowing agent loading. Solid (○); 2 phr blowing agent (●); 4 phr blowing agent (□); 6 phr blowing agent (△).

50 , and 100°C are 0.85 , 0.84 , 0.72 , and 0.55 , respectively. This means that the rate of decrease of storage modulus with density at higher temperature is less than at lower temperature.

The plots of relative storage modulus (the ratio of storage modulus of microcellular rubber, E'_r , and storage modulus of solid rubber, E'_s) of 40 phr Vulcan XC 72-filled solid and closed cell microcellular vulcani-

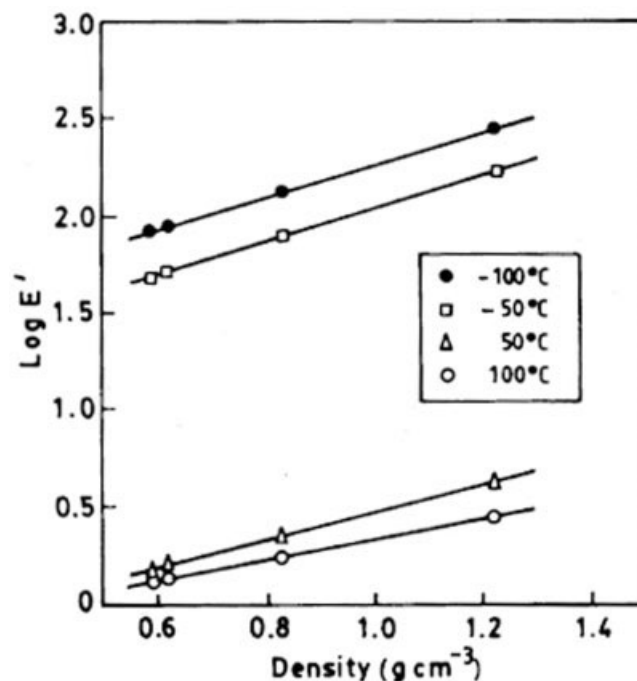


Figure 3 Plots of storage modulus versus density of 40 phr Vulcan XC 72-filled microcellular oil-extended EPDM vulcanizates at different temperatures.

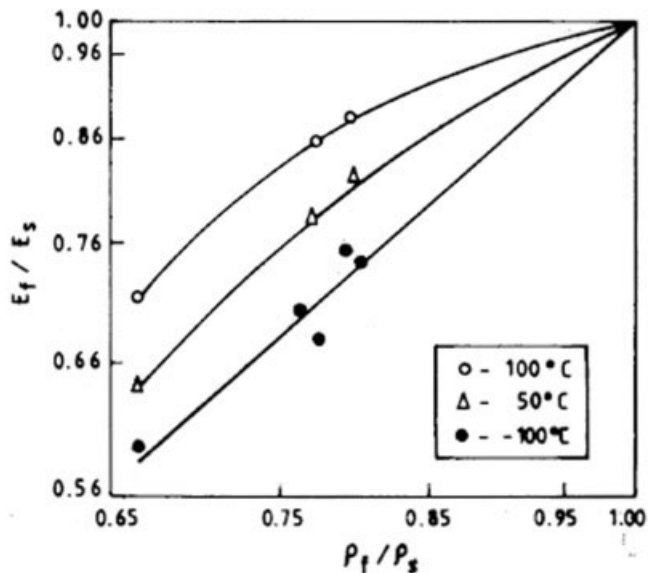


Figure 4 Plots of relative storage modulus (E_f/E_s) versus relative density (ρ_f/ρ_s) at different temperatures.

zates at three different temperatures, that is, -100 , 50 , and 100°C are shown in Figure 4. It shows that the relative storage modulus decreases at all the three temperatures with decrease in relative density (the ratio of density of microcellular rubber, ρ_f , and density of solid rubber, ρ_s). It is also observed that the relative storage modulus of closed cell microcellular rubber shows a higher value with increase in temperature for any relative density.

The variation of loss tangent ($\tan \delta$) with temperature for 40 phr Vulcan XC 72-filled solid and closed cell microcellular vulcanizates is shown in Figure 5. It exhibits the damping behavior of closed cell microcel-

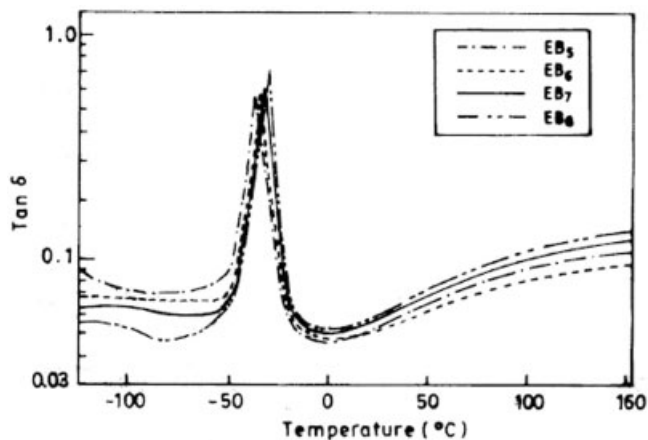


Figure 5 Plots of loss tangent ($\tan \delta$) versus temperature of 40 phr Vulcan XC 72-filled microcellular oil-extended EPDM vulcanizates: Effect of blowing agent loading. Solid (\cdots); 2 phr blowing agent ($---$); 4 phr blowing agent ($---$); 6 phr blowing agent ($- \cdot - \cdot -$).

TABLE II
Glass Transition Temperatures (T_g) of 40 phr Vulcan XC 72-Filled Microcellular Oil-Extended EPDM Vulcanizates

	EB ₅	EB ₆	EB ₇	EB ₈
T_g ($^\circ\text{C}$)	-37.5	-36	-34.5	-32.5
$\tan \delta$	0.68	0.70	0.74	0.82

lular vulcanizates, with variation of blowing agent loadings. $\tan \delta$ values corresponding to the glass transition temperature (T_g), i.e., the temperature at which the peak occurs are shown in Table II. T_g of all systems is very close. The higher $\tan \delta$ at higher blowing agent loading may be due to induced strain by decomposed gas pressure. In rubbery region, i.e., above 25 – 30°C , the $\tan \delta$ values decreases at lower blowing agent loading up to 2 phr. Whereas at higher blowing agent loading, that is, at 6 phr $\tan \delta$ values increases. It is because the enclosed gas in closed cell has little contribution toward the damping property.¹ For closed cell microcellular rubber at a higher blowing agent loading, the decomposed gas pressure increases inside the cell.²⁶ But in case of open cell, the damping behavior is largely affected by the viscosity of the fluid.⁷ Owing to the increase in decomposed gas pressure, the cell membrane remains in a strained condition. This increase in strain increases the $\tan \delta$ value, i.e., damping to some extent. This is also observed in strain-dependent dynamic mechanical properties.

Effect of frequency

The storage modulus (E') of Vulcan XC 72-filled microcellular rubber vulcanizates at four frequencies (f) of 3.5, 11, 35, and 110 Hz, and at a temperature range from 30 to 160°C is plotted in Figures 6–9. All data were taken on a single specimen. These data were

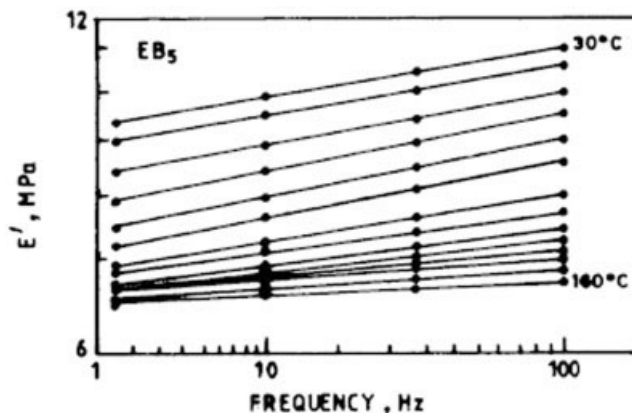


Figure 6 Plots of storage modulus (E') versus frequency at temperatures ($>T_g$) of 40 phr Vulcan XC 72-filled solid oil-extended EPDM vulcanizates.

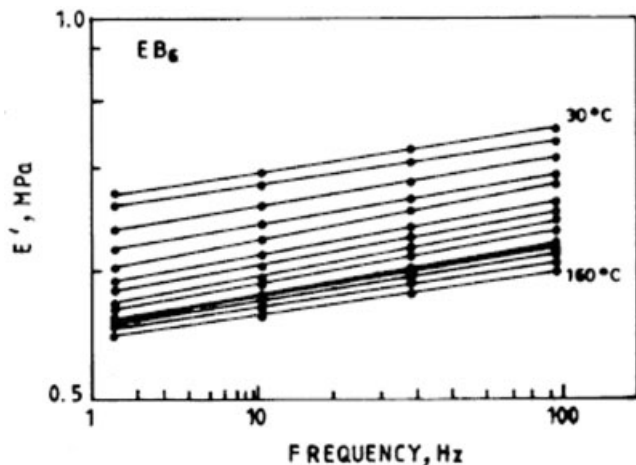


Figure 7 Plots of storage modulus (E') versus frequency at temperatures ($>T_g$) of 40 phr Vulcan XC 72-filled 2 phr blowing agent-loaded microcellular oil-extended EPDM vulcanizates.

obtained to define the time-temperature dependence of the modulus of microcellular rubber. A logarithmic plot of E' versus frequency shows that the storage modulus is strain rate-dependent and increases with frequency at all temperatures. Also, the rate dependence decreases at high temperatures. The curves were shifted along the frequency axis to obtain superposition. The resulting shift factors ($\log a_T$) at any temperature for the storage modulus were obtained with respect to room temperature (30°C). The $\log a_T$ values are plotted against $10^3/T$ in Figure 10, and the activation energy (ΔH) value is calculated by using Arrhenius equation:^{22,23}

$$\log a_T = \frac{\Delta H}{2.303R} \left(\frac{1}{T} - \frac{1}{T_0} \right) \quad (2)$$

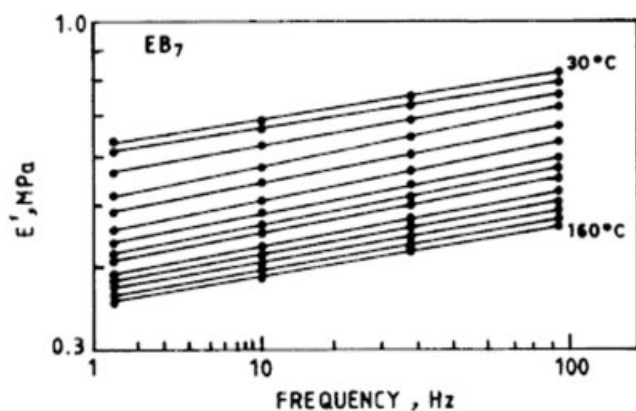


Figure 8 Plots of storage modulus (E') versus frequency at temperatures ($>T_g$) of 40 phr Vulcan XC 72-filled 4 phr blowing agent-loaded microcellular oil-extended EPDM vulcanizates.

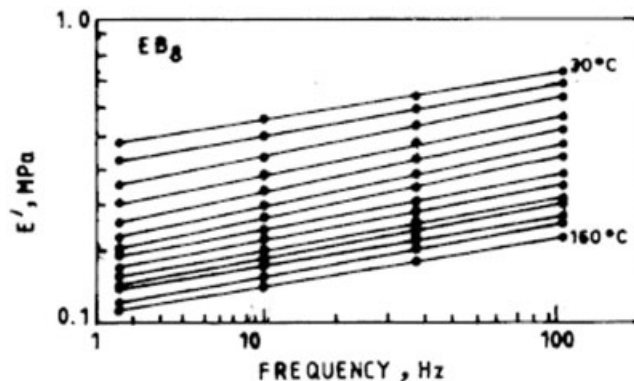


Figure 9 Plots of storage modulus (E') versus frequency at temperatures ($>T_g$) of 40 phr Vulcan XC 72-filled 6 phr blowing agent-loaded microcellular oil-extended EPDM vulcanizates.

where T_0 is the reference temperature, i.e., 303 K, $\log a_T$ is the shift factor (i.e., zero when T is T_0), ΔH is the activation energy (i.e., flow activation energy) in calories/mole, and R is the gas constant (1.9872 cal/(mol K)). From Figure 10, the slope of the straight-line, i.e., ΔH values, is calculated for both solid and microcellular rubber. ΔH value for the solid was found to be 22.4 kcal/mol, whereas the ΔH for the microcellular rubber was nearly equal to 14 kcal/mol.

The data from Figures. 6-9 are replotted in Figure 11 as E' versus $\log fa_T$, using a_T from the Arrhenius

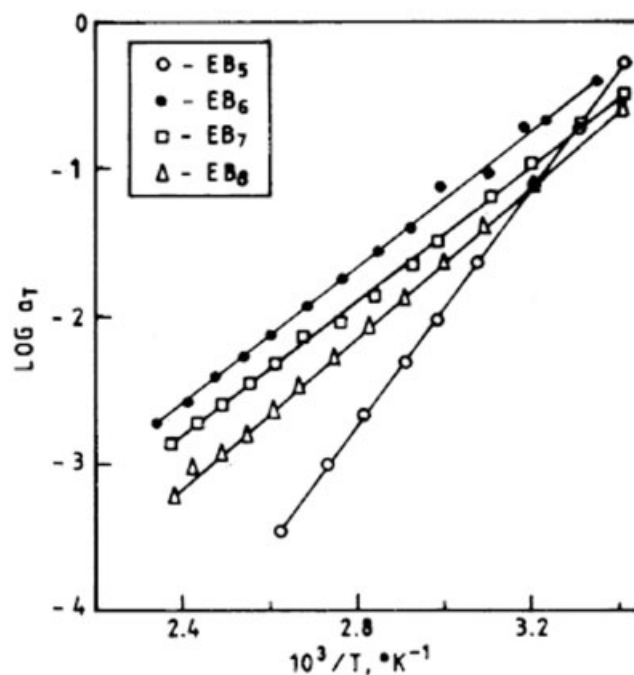


Figure 10 Plots of $\log a_T$ versus temperature 40 phr Vulcan XC 72-filled solid and microcellular oil-extended EPDM vulcanizates. Solid (\circ); 2 phr blowing agent (\bullet); 4 phr blowing agent (\square); 6 phr blowing agent (\triangle).

equation, with f being the frequency in cycles per second, to obtain the master curves of $\log E'$ versus $\log fa_T$ corresponding to the microcellular EPDM rubbers and the solid vulcanizate. The curves represent the storage modulus of these materials at 30°C. Construction of master curves implies that the storage modulus of solid and microcellular oil-extended EPDM follow the time-temperature correspondence principle.

Figure 12 shows the plots of loss tangent with temperature for 6 phr blowing agent-loaded microcellular rubber, at four frequencies of 3.5, 11, 35, and 110 Hz. Below T_g , the $\tan \delta$ value decreases with the decrease in frequency. The T_g decreases and shifts toward right i.e., shifts toward high temperature with increase in frequency. However, above T_g and up to 50°C the $\tan \delta$ value decreases with increase in frequency. At higher temperature, the trend is reversed due to the "pseudorigidity" phenomenon i.e., effect of frequency.²⁷ In this effect, the relaxation time responsible for the chain mobility reduces drastically with increase in frequency and, as a result, the amorphous chain temporarily freezes. This effect is minimized at high temperature and the trend is reversed. Similar results were also obtained at other loadings of blowing agent.

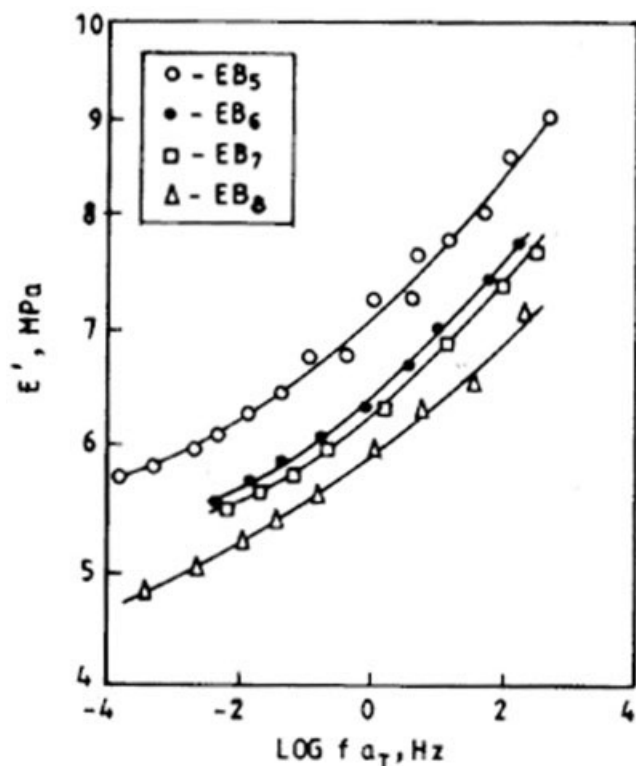


Figure 11 Master curves of storage modulus (E') of solid and microcellular rubber vulcanizates. Solid (○); 2 phr blowing agent (●); 4 phr blowing agent (□); 6 phr blowing agent (△).

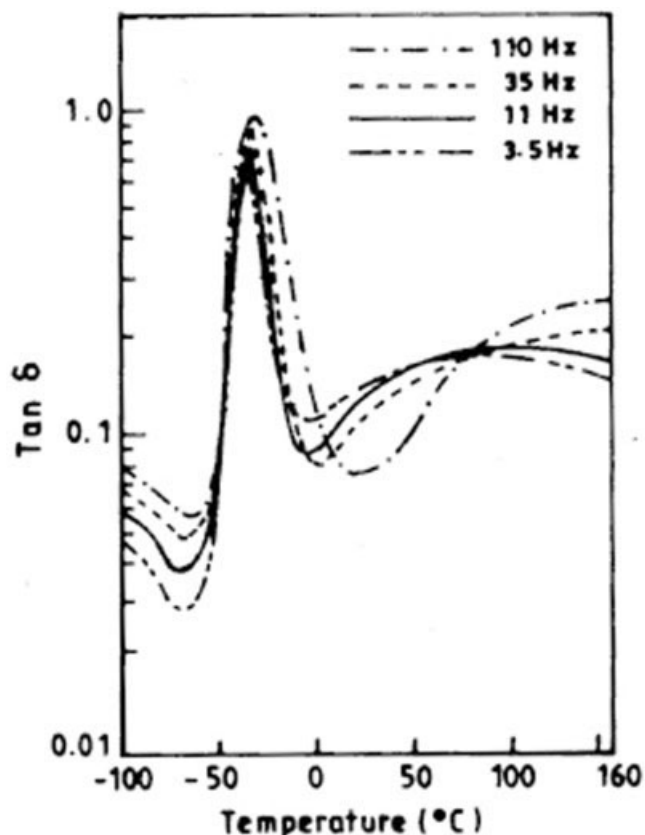


Figure 12 Plots of loss tangent ($\tan \delta$) versus temperature of 40 phr Vulcan XC 72-filled and 6 phr blowing agent-loaded microcellular oil-extended EPDM vulcanizates: Effect of frequency. 110 Hz (- · - · -); 35 Hz (- - -); 11 Hz (—); 3.5 Hz (— — —).

Strain-dependent dynamic mechanical properties

Storage modulus

Figure 13 shows the effect of strain and blowing agent on storage modulus of 40 phr Vulcan XC 72-filled solid and microcellular vulcanizates. At the lowest imposed strain amplitude, both solid- and closed-cell microcellular rubber vulcanizates show the highest storage modulus, E' . At the lowest DSA (0.08%), the three-dimensional polymer-filler, filler-filler, and entrapped decomposed gas (closed-cell) structures act as a rigid unit against the imposed strain, and hence it shows the highest modulus value. The low strain is not capable of causing any significant change in the network structure. Figure 13 shows that the absolute modulus value decreases with increase in blowing agent loading in 40 phr Vulcan XC 72-loaded closed-cell microcellular compounds at room temperature. The figure also shows the insensitivity to the strain effect below 1% DSA. With increase in blowing agent loading, the thickness of the cell membrane reduces and the stiffness of the compounds decreases, which results in the

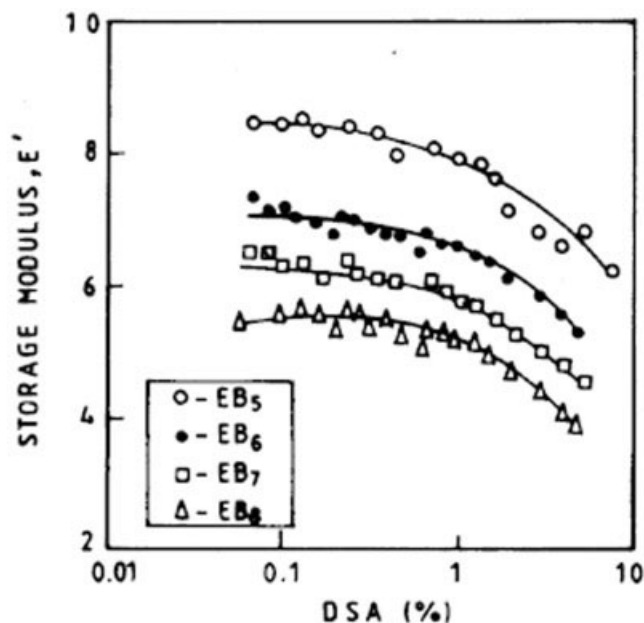


Figure 13 Storage modulus (E') as a function of DSA of 40 phr Vulcan XC 72-filled solid and microcellular oil-extended EPDM vulcanizates: Effect of blowing agent loading. Solid (\circ); 2 phr blowing agent (\bullet); 4 phr blowing agent (\square); 6 phr blowing agent (\triangle).

lower value of the storage modulus. The fall of storage modulus above 1% DSA is sharp with increasing strain. This is due to the collapse of a weak cell membrane with increase in strain amplitude.¹

Loss tangent

$\tan \delta$ versus DSA% plots of solid and microcellular vulcanizates of 40 phr Vulcan XC 72-loaded compounds with variation of the blowing agent are shown in Figure 14. It is observed that $\tan \delta$ value increases with the increase in the blowing agent loading at all strains. At lower strain, the loss tangent increases slowly with the increase in strain. In the closed-cell microcellular rubber, the bending, bucking, and extension of the cell membrane^{26,28} occur at low strain. Hence, the $\tan \delta$ value shows a higher value than do solid vulcanizates. In high-strain regions, i.e., above 1% DSA, the loss tangent value increases sharply due to the breakdown of the filler aggregates in the solid vulcanizates. Whereas, in the case of microcellular rubber, another factor (i.e., jamming and collapse of the cell membrane) plays an important role in increasing the $\tan \delta$.

Relationship between storage modulus and loss modulus

The relationship between storage modulus (E') and loss modulus (E'') for 40 phr loaded Vulcan XC 72-

filled closed-cell microcellular EPDM vulcanizates over a wide range of DSA from 0.08 to 7% is illustrated in Figure 15. The Cole-Cole plots^{15,22,23,29,30} of the complex dynamic modulus represent the amplitude dependence of its components E' and E'' . It is evident from the figure that the straight line for solid rubber vulcanizates and circular arc relationship holds good for the closed-cell microcellular rubber vulcanizates. Each point along the arc corresponds to different amplitude of vibration. It is seen that the circular arc decreases with increase in the blowing agent loading. At lower amplitude, the storage modulus shows a higher value as a result of the elastic buckling or extension of the cell walls of closed cell microcellular rubber.¹ Owing to the breakdown of some cell walls at higher amplitude, both storage and loss modulus decrease, which corresponds to the circular arc relationship.²⁸

Relationship between loss tangent and storage modulus

Medalia and Laube³¹ reported the following simple relation between $\tan \delta$ and storage modulus for natural rubber at 10% DSA at 25°C:

$$\tan \delta = 0.033 + 0.0449(E'_{1\%} - E'_{10\%})^{1/2} \quad (3)$$

Even it is mathematically defined for the model system that the dynamic mechanical properties of polymeric system may show different types of dependence with one another, especially when fillers are incorporated. A linear relationship between $\tan \delta$ and $\log E'$ was also established by Namboodiri et

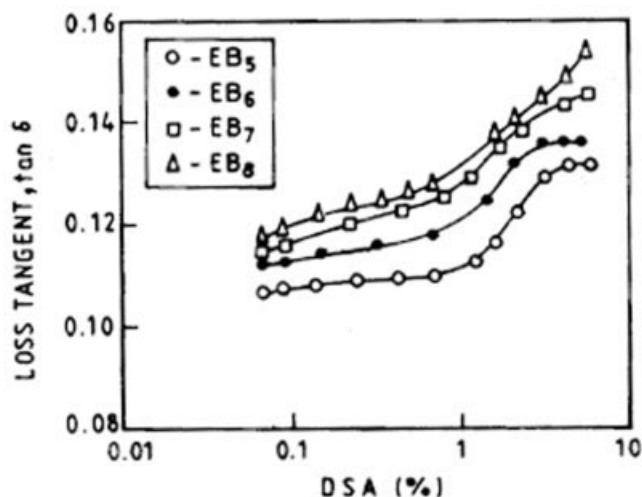


Figure 14 Loss tangent ($\tan \delta$) as a function of DSA of 40 phr Vulcan XC 72-filled solid and microcellular oil-extended EPDM vulcanizates: Effect of blowing agent loading. Solid (\circ); 2 phr blowing agent (\bullet); 4 phr blowing agent (\square); 6 phr blowing agent (\triangle).

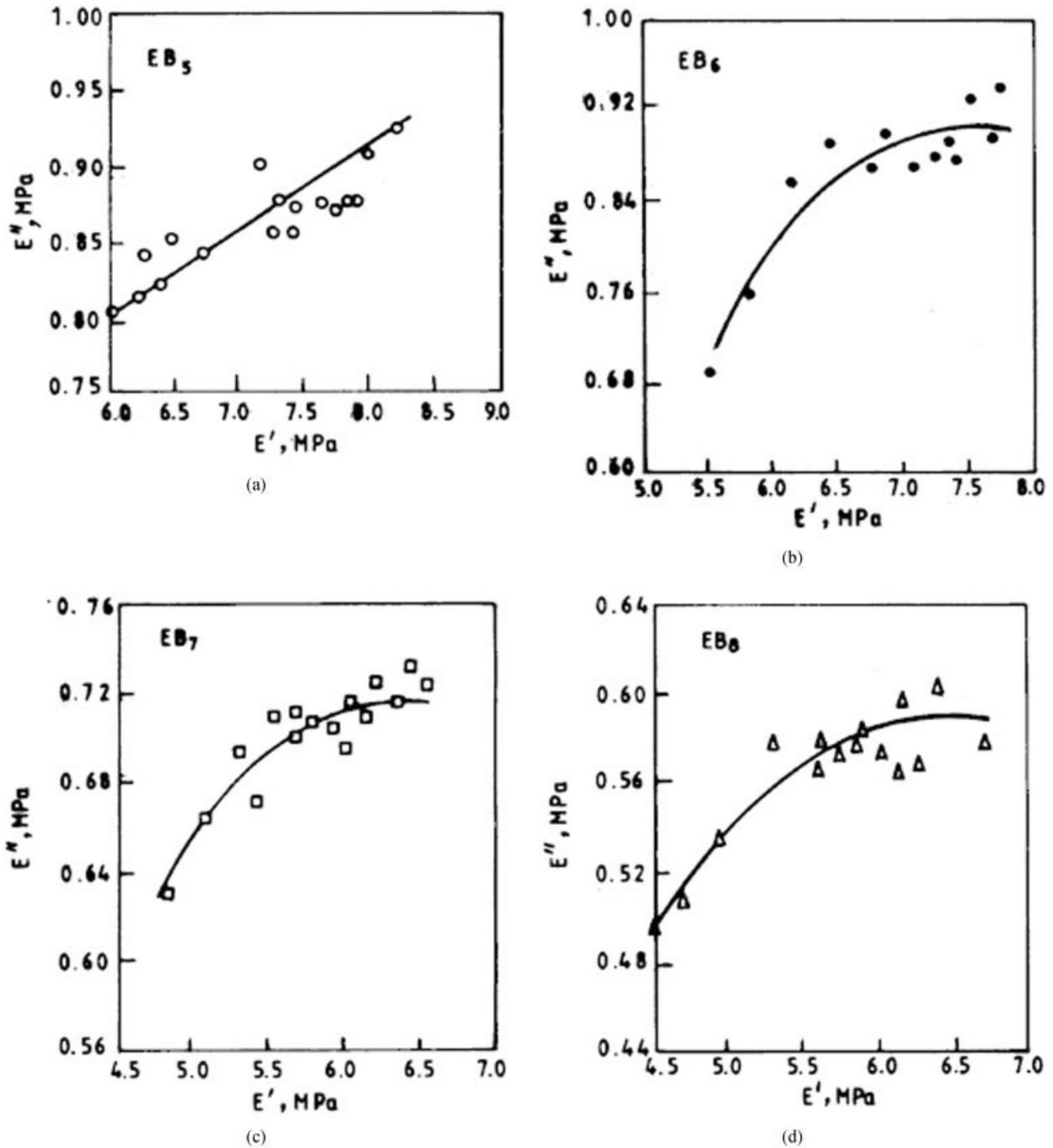


Figure 15 E' and E'' relationships of 40 phr Vulcan XC 72-filled solid and microcellular oil-extended EPDM vulcanizates: Effect of variation in blowing agent loadings. (a) solid (b) 2 phr blowing agent (c) 4 phr blowing agent, and (d) 6 phr blowing agent.

al.¹⁸ for carbon black-filled EPDM vulcanizates. Figure 16 shows the plot of $\tan \delta$ as a function of $\log E'$ for 40 phr Vulcan XC 72-filled closed-cell microcellular EPDM vulcanizates, with variation of blowing agent loading (density). The linear nature of the plot could be mathematically expressed as follows:

$$\tan \delta = m \log E' + C$$

where m is the slope of the line and C is a constant. With incorporation of the blowing agent, the slope (m) increases compared to the solid rubber vulcanizates, but with variation of the blowing agent loading, the slope remains almost unchanged. The existence of such a relation when a purely hysteric parameter is related to a purely elastic parameter shows that the primary cause is most probably the filler-filler inter-

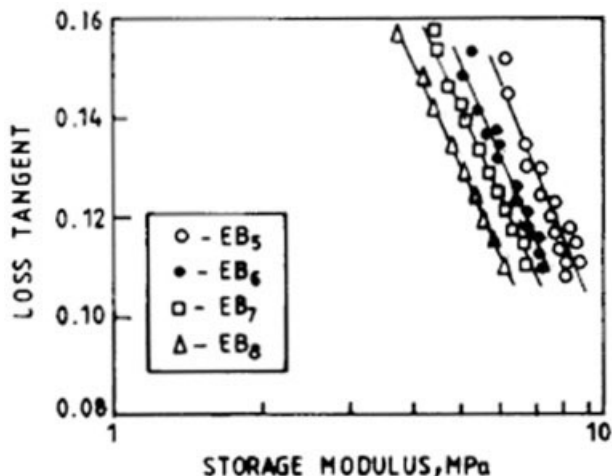


Figure 16 Plots of loss tangent ($\tan \delta$) versus storage modulus (E') of 40 phr Vulcan XC 72-filled solid and microcellular oil-extended EPDM vulcanizates. Solid (○); 2 phr blowing agent (●); 4 phr blowing agent (□); 6 phr blowing agent (△).

action and the deformation of entrapped air inside the closed cell.¹

CONCLUSIONS

1. The storage modulus (E') or stiffness of microcellular EPDM (oil-extended Keltan 7341A) reinforced with Vulcan XC 72 decreases concomitantly with increase in blowing agent loading. Plot of $\log E'$ versus density shows the linear relationship at all temperatures. With increase in temperature, the slope decreases, and so the rate of decrease of storage modulus with density increases.
2. The relative storage modulus (E'_r/E'_g) decreases with decrease in relative density (ρ_f/ρ_s). With increase of temperature, the relative storage modulus shows a higher value for all values of density.
3. In glassy region, loss tangent ($\tan \delta$) value of Vulcan XC 72-loaded oil-extended EPDM microcellular rubber vulcanizates increases with increase in blowing agent loading in rubbery region at lower blowing agent loading. $\tan \delta$ value decreases at higher blowing agent loading, and again it increases due to increase of decomposed gas pressure inside the cell.
4. The storage modulus is found to be frequency- or strain rate-dependent. The storage modulus increases with increase in frequency for all temperatures. Modulus versus log-reduced strain rate master curves are formed by a time-temperature superposition method, by using shift factors calculated from Arrhenius equation for both solid and microcellular Keltan 7341A EPDM rubber.
5. The loss tangent values decreases with decrease of frequency in glassy region. Around 40°C, the $\tan \delta$ value decreases due to temporary freezing of chains occurring at high frequency. At higher temperature, the trend is reversed due to the effect of frequency called as "pseudorigidity" phenomenon.
6. The storage modulus of 40 phr Vulcan XC 72-filled microcellular Keltan7341A vulcanizates decreases slowly with increase in blowing agent loading below 1% DSA. Whereas at higher DSA i.e., above 1% storage modulus, it drops sharply for both solid and microcellular rubber. Exactly a reversed trend occurs in case of loss tangent i.e., below 1% DSA slow increase and above 1% increases sharply.
7. The plots of storage modulus versus loss modulus for 40 phr Vulcan XC 72-filled microcellular Keltan 7341A EPDM rubber vulcanizates exhibit a circular arc relationship, which decreases with increase of blowing agent loading.
8. Storage modulus and loss tangent shows a linear relationship, the slope of which is independent of blowing agent loading.

References

1. Guriya, K. C.; Tripathy, D. K. *J Appl Polym Sci* 1996, 61, 805.
2. Kujawa, F. M. *J Cell Plast* 1965, 1, 400.
3. Briscoll, H.; Thomas, C. R. *British Plastics*, 1968, p 79.
4. Turner, R. B.; Spell, H. L.; Wilkes, G. L. *Proc SPI 28th Ann Tech Market Conf* 1984, 224.
5. Kosten, C. W.; Zwickwer, C. *Rubber Chem Technol* 1939, 12, 105.
6. Gent, A. N.; Rusch, K. C. *J Cell Plast* 1966, 2, 46.
7. Gent, A. N.; Rusch, K. C. *Rubber Chem Technol* 1966, 39, 389.
8. Rinde, J. A.; Hoge, K. G. *J Appl Polym Sci* 1971, 15, 1377.
9. Rinde, J. A.; Hoge, K. G. *J Appl Polym Sci* 1972, 16, 1409.
10. Jackson, C. L.; Show, M. T.; Auburt, J. H. *Polymer* 1991, 32, 221.
11. Payne, A. R. *J Appl Polym Sci* 1964, 8, 266.
12. Payne, A. R. *J Appl Polym Sci* 1964, 7, 873.
13. Payne, A. R. *Rubber Chem Technol* 1964, 37, 1190.
14. Sircar, A. K.; Lamond, T. G. *Rubber Chem Technol* 1975, 48, 79.
15. Dutta, N. K.; Tripathy, D. K. *Kautsch Gummi Kunstst* 1989, 42, 665.
16. Byrne, L. F.; Hourston, D. J. *J Appl Polym Sci* 1979, 23, 16.
17. Byrne, L. F.; Hourston, D. J. *J Appl Polym Sci* 1979, 23, 2899.
18. Namboodiri, C. S. S.; Tripathy, D. K.; Salinkar, P. L. *Kautsch Gummi Kunstst* 1992, 43, 770.
19. Hazlton, D. R.; Puydak, R. C. *Rubber Chem Technol* 1971, 44, 1043.
20. Namboodiri, C. S. S.; Tripathy, D. K. *Plast Rubber Compos Process Appl* 1992, 17, 171.
21. Nayak, N. C.; Tripathy, D. K. *Plast Rubber Compos Process Appl* 2001, 30, 1.
22. Nayak, N. C.; Tripathy, D. K. *Kautsch Gummi Kunstst* 2005, 58, 50.
23. Nayak, N. C.; Tripathy, D. K. *Cell Polym* 2001, 20, 386.
24. Mahapatra, S. P.; Tripathy, D. K. *Cell Polym* 2004, 23, 127.
25. Mahapatra, S. P.; Tripathy, D. K. *Cell Polym* 2005, 24, 30.
26. Gibson, L. J.; Ashby, M. F. *Cellular Solids, Structure and Properties*; Pergamon: Oxford, 1988.
27. Boyer, R. F. *J Polym Sci Part C: Polym Symp* 1996, 14, 267.
28. Guriya, K. C.; Tripathy, D. K. *J Elast Plast* 1995, 27, 305.
29. Mukhopadhyay, K.; Tripathy, D. K.; De, S. K. *J Appl Polym Sci* 1993, 48, 1089.
30. Mukhopadhyay, K.; Tripathy, D. K. *J Elast Plast* 1993, 24, 203.
31. Medalia, A.; Laube, S. G. *Rubber Chem Technol* 1978, 51, 89.